JOURNAL OF MATERIALS SCIENCE 20 (1985) 1445–1454

The influence of molecular weight on the fracture of thermoplastic glassy polymers

P. PRENTICE*
Department of Mechanical Engineering, Imperial College of Science and Technology, London SW7 2BX, UK

Experimental evidence is presented in support of a previously proposed relationship between the fracture energy of glassy polymers and the square of the molecular weight. The critical energy release per unit area of crack, G_c, has been found to fit the curve of the equation $G_c = Ax(M - M_e)^2 + (1 - x)B$, where $x = 1$ for molecular weights below some critical value M_c and x tends to zero for $M > M_c$, and it is suggested that x is some measure of the extent of chain "pull-out" during fracture. This implies that for $M > M_c$, chain scission becomes increasingly dominant. A linear correlation is also predicted between the critical crack opening displacement (COD) and the molecular weight below M_c.

1. Introduction

The early work of Berry [1, 2] highlighted the fact that in polymeric materials, the measured fracture surface energy is very much higher than that obtained from the calculation of the energy necessary to break all molecular chains crossing unit area of a plane perpendicular to an applied stress. The increase has been attributed to a local ductile response of the material under the influence of the high stresses at the crack tip.

In their unstressed state, isotropic glassy polymers have been shown to consist of separate chain-like entities in the form of random coils [3]. In this configuration, scission of a chain due to the application of an external stress is not possible. Before scission can occur, regions of the chain must first be extended to their ultimate elongation. An additional requirement for chain scission in this way is that the ends of the elongated segment are securely held, otherwise the whole chain will be expected to slip.

It is now generally accepted that the strength of glassy polymers is related to the long-range interconnectiveness of entanglement points [4, 5]. The nature of the entanglements is not well understood, although, in a previous paper [6], it was argued that a popularly held view of an entanglement acting like a knot is unlikely because of the inflexibility of the chains imposed by substituents on the main chain and the small aspect ratio of the chain segment in the vicinity of the entanglement point. A model was proposed in which the motion of the chains is restricted by the proximity of their neighbours, effectively preventing any lateral movement. Movement in the axial direction of the chain is also inhibited by the presence of polar side-groups on the chain which interact with those on other molecules.

It was proposed, using a model for the removal of a polymer chain through an imaginary "tube", that below some critical molecular weight (M_c) the fracture energy was proportional to the square of the molecular weight. Above M_c, the fracture energy became independent of the molecular weight. The object of the present work is to advance experimental evidence in support of this proposal.

2. The entanglement concept

It is now widely accepted that the rigidity of

Present address: Institut Algerien du Petrole, B.P. 103, Annaba, Algeria.

0022–2461/85 $03.00 + .12

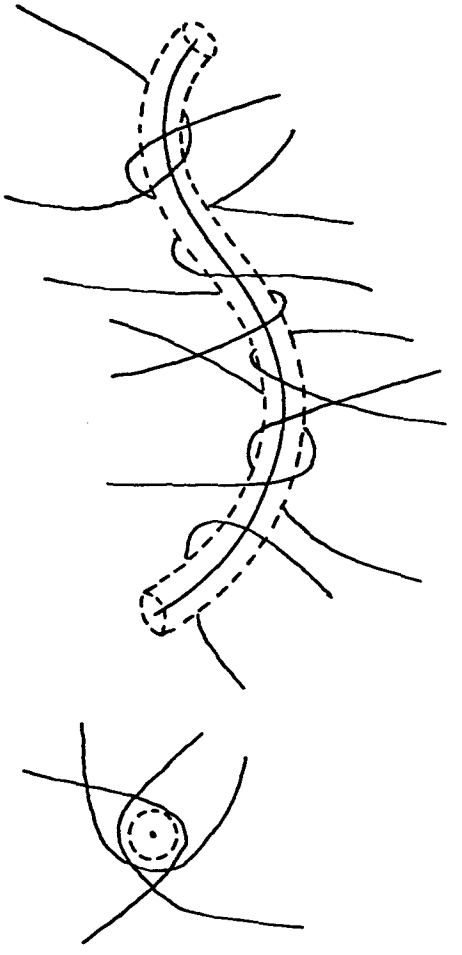

Figure 1 Idealized model of a chain in a three-dimensional network, depicting the "tube" created by the presence of neighbouring chains.

amorphous glassy polymers at ambient temperatures is related to the degree of entanglement of the polymer chains of which they are composed. The mobility of the chains is severely restricted by the presence of these entanglements since, in moving, one molecule may not cross the contour of another [7]. Longitudinal motion is also inhibited by the interaction of substituents on neighbouring chains, producing potential barriers to chain mobility. These potential barriers are assumed to occur at regular intervals along the chain [8]. In the case of polymethylmethacrylate (PMMA), for example, the high electron density of the ester side-groups contributes to the immobility. So, the presence of entanglements effectively prevents any lateral motion of the chains and any movement is restricted to a direction governed by an imaginary tube formed around a chain by the proximity of its neighbours (see Fig. 1).

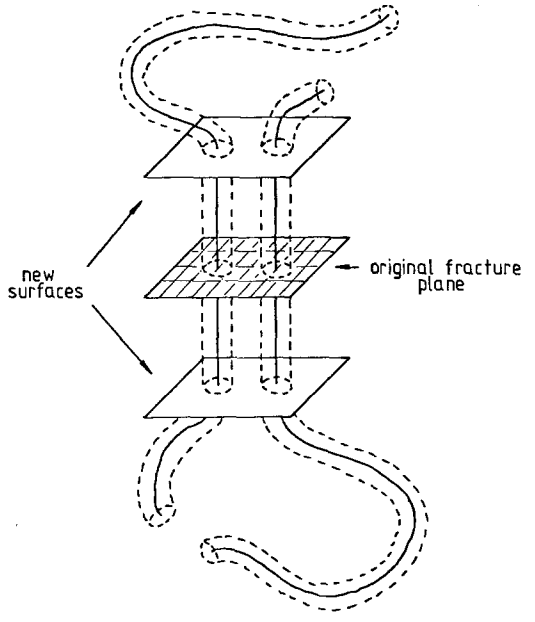

Figure 2 Schematic representation of the "pull-out" process in the formation of new surfaces during crazing.

3. Crack propagation

It is well established that in PMMA, as in other glassy polymers, the propagating crack is preceded by a craze which opens without weakening [9] by a mechanism in which material is drawn into it from the newly formed surface. A review by Kinloch [10] and the extensive contributions of Donald and Kramer (see for example [11–13]) describe the current understanding of the micromechanisms of crack extension in polymers. The drawing process may be modelled as in Fig. 2; the polymer chains in an unstressed isotropic sample are embedded in both sides of the plane of a propagating crack. As the crack opens, one portion of the chain will be removed from the bulk of the specimen into the region between the new surfaces. It is only necessary for this to happen on one side of the plane, that containing the shorter length of chain.

Usually, at temperatures below the glass transition temperature (T_g), chain mobility is effectively prevented by the high entanglement density and restricted rotation about the main chain bonds. In order that viscoelastic deformation may occur and enable polymer chains to be drawn into the craze, it may be necessary to propose a situation in which chain mobility is enhanced. One theory put forward by Gent and Thomas [14, 15] proposed that devitrification of a small amount of material at the tip of a crack takes

place under the influence of a dilatant stress; this devitrification would allow the drawing process to occur.

However, a more likely explanation is that the high stresses prevailing at the crack tip during failure are sufficient to overcome the resistance to rotation about the main chain bonds and so give rise to a ductile failure mechanism for the material in this region [16], thus enabling a drawing process to take place.

4. Removal of chains into the craze layer

The motion of a polymer chain in a polymer melt or concentrated solution has been described by the concept of reptation [17, 18], in which the chain is proposed to move along an imaginary tube in a worm-like manner. Similarly, the removal of polymer chains during fracture may be modelled using a tube concept.

Based on a simple power-law viscous model, as shown schematically in Fig. 3, the shear stress (τ) experienced by the chain in its tube will be proportional to the apparent strain rate, $\dot{\gamma}_a$, i.e.

$$\tau = \mu(\dot{\gamma}_a)^n \tag{1}$$

where μ is a coefficient of viscosity resulting from the interaction of the substituents on neighbouring chains, and n is the power-law index; but:

$$\tau = \frac{f}{A} \tag{2}$$

where f is the force acting on the end of the chain in the tube direction, and A is the effective surface area of the chain:

$$A = 2\pi rl \tag{3}$$

r being the radius of the chain, and l is the contour length of the tube remaining occupied.

The apparent strain rate may be defined by:

$$\dot{\gamma}_a = \frac{v}{h} \tag{4}$$

where h is the spatial gap between the chain and the surface of its imaginary tube, and v is the rate of removal of the chain.

Combining Equations 1 to 4, we obtain:

$$f = \mu 2\pi r\left(\frac{v}{h}\right)^n l \tag{5}$$

that is, at constant v, the force acting on the chain in the tube direction is proportional to the length of the tube remaining occupied. The energy

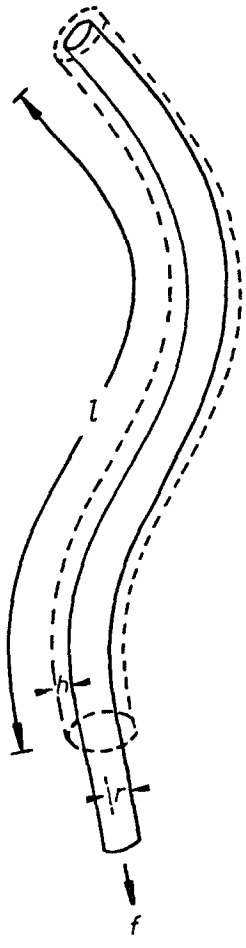

Figure 3 Schematic representation of the mechanism of chain removal.

required to remove one chain from its tube:

$$\Gamma_0 = \int_{l=0}^{l=L} f\,dl \tag{6}$$

where L is the total length of the tube vacated, i.e.

$$\Gamma_0 = \int_{l=0}^{l=L} \mu 2\pi r\left(\frac{v}{h}\right)^n l\,dl \tag{7}$$

so that at constant v:

$$\Gamma_0 = \mu\pi r\left(\frac{v}{h}\right)^n L^2 \tag{8}$$

The work done per unit area of plane will then be:

$$\Gamma = \Gamma_0 a \tag{9}$$

where a is the number of segments crossing unit area of plane and, in this analysis is assumed to be a function of the molecular cross-sectional area only [19].

The problems presented by the possibility of multiple crossings of chains through the fracture plane are ignored in the current work. This is because the molecular weights of interest are low, combined with the assumption that polymer chains such as PMMA, having two bulky side groups per repeat unit, are reasonably rigid and unlikely to fold back on themselves to any great degree. Hence combining Equation 8 and 9:

$$\Gamma = \mu\pi ra\left(\frac{v}{h}\right)^n L^2 \tag{10}$$

This means that at a constant crack opening velocity, v, the work done in removing chains from a plane of unit area is proportional to the square of the molecular weight, since the length of a polymer chain and its associated tube is directly proportional to its molecular weight, i.e.

$$\Gamma \alpha M^2 \tag{11}$$

The bonds in a fully extended segment may only withstand a finite stress before failing by homolytic scission and a consequence of Equation 5 is that at a constant crack opening velocity, a critical value of the force (f_c) will be reached at some critical chain length (l_c). Below this critical length, the chains will fail by a pull-out mechanism and the fracture energy will be determined by Equation 10. However, above l_c, the force necessary to initiate a pull-out mechanism will be greater than that which the individual links in the chain are able to withstand. In this case, scission becomes the sole mechanism for chain failure, and the fracture energy is expected to be independent of the molecular weight.

5. Fracture mechanics

Linear elastic fracture mechanics (LEFM) has been used extensively with polymeric materials and has been found to satisfactorily describe the brittle failure of PMMA [20], since the strain at failure is small and still within the elastic limit of the material.

The basic equation used relates the stress intensity factor, K, to the applied stress, σ, on a large plate containing a central flaw of length $2c$. The theory predicts that failure will occur when:

$$\sigma^2\pi c = K_c^2 \tag{12}$$

where K_c is the critical stress intensity factor, or the fracture toughness. A value of y^2, a geometry function, may be substituted for π when different geometries are employed.

If artificial flaws of length c are introduced into one edge of a series of test specimens, a plot of $\sigma^2 y^2$ against $1/c$ results in a straight line with a slope of K_c^2. For linear elasticity, K_c is related to G_c (the critical energy released per unit of crack growth) by [20]:

$$K_c^2 = E^* G_c \tag{13}$$

where E^* is the modulus, which is equal to Young's modulus, E, for plane stress and $E/(1 - \nu^2)$ in plane strain, where ν is Poissons's ratio. (The error introduced by neglecting the correction factor for plane strain is small, so in the current work is ignored.)

As defined by Equation 10, Γ is the fracture energy per unit area of plane and, as such, is equivalent to G_c, so that:

$$\Gamma = G_c \tag{14}$$

The fracture stress used in Equation 12 was calculated from [21]:

$$\sigma = \frac{3PS}{2bd^2} \tag{15}$$

where σ is the fracture stress in the outer fibres at the midspan of a specimen tested in three-point bending; P is the load at fracture, S is the support span length, b is the beam width, and d is the beam depth. Similarly, the modulus was found from [21]:

$$E = \frac{S^3 m}{4bd^3} \tag{16}$$

where m is the slope of the tangent to the straight-line portion of the load–deflection curve.

6. Material and specimen preparation

The material used in this study was an ICI Perspex grade of PMMA supplied in 6 mm thick sheet form. All specimens were machined from a single 2.4 m × 1.2 m sheet to the dimensions shown in Fig. 4. A total of 112 specimens were made and separated into 14 sets of 8 specimens. Into each specimen of the set, a single notch, ranging in length from 1.5 to 11.5 mm, was introduced using a fly cutter with a tip radius of 12 μm. Each complete set was exposed to γ-radiation from a Cobalt-60 source, having a nominal dose rate of 0.7 Mrad h^{-1}, for different lengths of time, as in Table I.

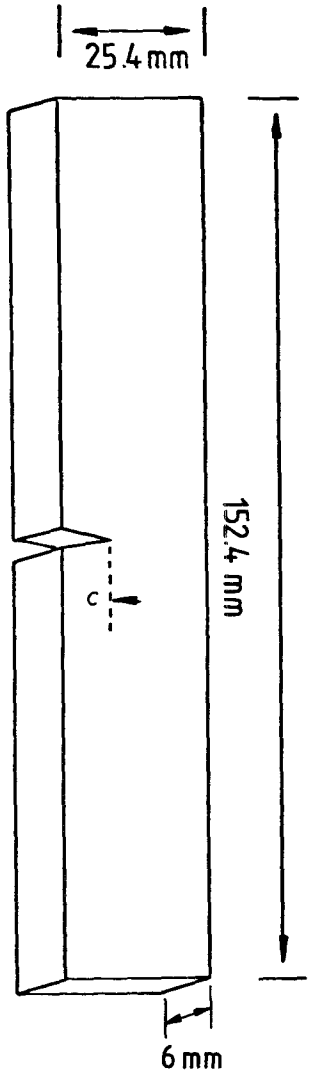

Figure 4 Three-point bend test specimen dimensions.

7. Molecular weight

Since PMMA is unusual in that it is degraded by γ-radiation without appreciable crosslinking [22], it is possible to calculate the number average molecular weight, $\bar{M}_n$, from a known value before irradiation using the following equation [23]:

$$\frac{1}{\bar{M}_n} = \frac{1}{\bar{M}_n(0)} + \left(\frac{R \times G_f}{9.6}\right) 10^{-5} \qquad (17)$$

where R is the total dose in Mrad, G_f is the number of chain scissions per 100 eV of absorbed energy (G_f for PMMA = 1.7) [23], and $\bar{M}_n(0)$ is the initial molecular weight.

In the present work, however, it was decided not to rely on the calculated values of $\bar{M}_n$, but to measure the molecular weight of each set independently using gel permeation chromatography (GPC). This was performed by the Polymer Supply and Characterisation Centre at the Rubber and Plastics Research Association, using tetrahydrofuran as the eluting solvent at 35° C. Independent verification of the molecular weight has the added advantage of yielding molecular weight averages other than the number average.

The nature of the polymerization process results in the fact that chains of varying length are produced and that the molecular weight measured by all techniques is actually an average value. Apart from the number average, three other quantities are commonly quoted: the weight average, $\bar{M}_w$, the so-called z-average, $\bar{M}_z$, and the viscosity average M_v. The different values are defined as follows:

TABLE I

Sample set	Irradiation time (h)	$\bar{M}_n$ (× 10^{-6})	$\bar{M}_z$ (× 10^{-6})	$\bar{M}_z/\bar{M}_n$	K_c (MN $m^{-3/2}$)	G_c* (J m^{-2})	E (GN m^{-2})
A	0.0	0.35	4.36	12.4	1.79	1068	3.07
B	0.5	–	–	–	1.84	1128	2.88
C	1.0	0.24	1.30	5.4	1.90	1203	3.00
D	2.0	–	–	–	1.89	1190	3.07
E	4.0	0.095	0.42	4.4	1.88	1178	2.95
F	8.0	0.065	0.26	4.0	1.84	1128	3.07
G	10.15	0.060	0.22	3.7	1.72	986	–
H	12.58	0.051	0.18	3.5	1.39	644	–
I	16.0	0.036	0.14	3.9	1.35	607	3.07
J	20.0	0.035	0.12	3.4	1.01	340	–
K	21.8	0.032	0.11	3.4	0.89	246	–
L	32.0	0.018	0.064	3.5	0.53	94	3.00
M	32.58	0.023	0.067	2.9	0.43	62	–
N	44.12	0.017	0.054	3.1	0.38	48	–

*In the calculation of G_c, the modulus, E, is assumed to be constant at 3.0 GN m^{-2}.

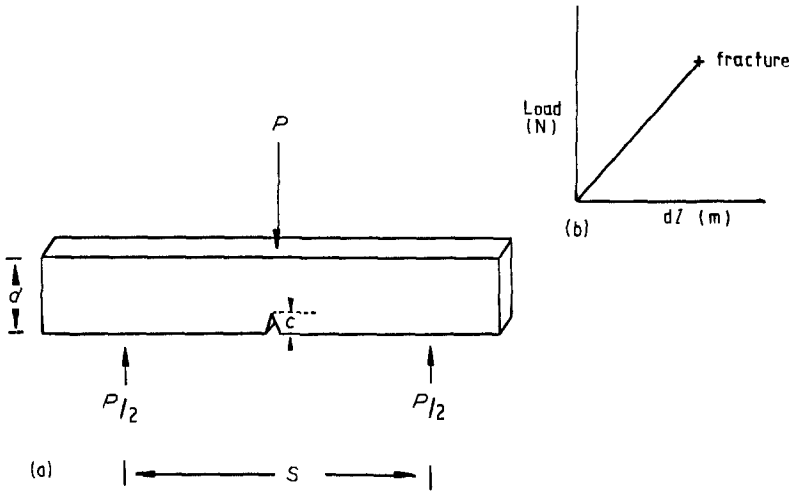

Figure 5 (a) Loading in three-point bend. (b) The inset shows a typical load–deflection curve.

$$\bar{M}_n = \frac{\Sigma n_i M_i}{\Sigma n_i} \quad (18a)$$

$$\bar{M}_w = \frac{\Sigma n_i M_i^2}{\Sigma n_i M_i} \quad (18b)$$

$$\bar{M}_z = \frac{\Sigma n_i M_i^3}{\Sigma n_i M_i^2} \quad (18c)$$

$$\bar{M}_v = \left(\frac{\Sigma n_i M_i}{\Sigma n_i M_i}\right)^{1+\alpha} \quad (18d)$$

where n_i is the number of molecules of molecular weight, M_i, Σ denotes summation over all i molecular weights, and the exponent α usually lies between 0.5 and 0.8 and is determined independently for each particular polymer/solvent combination.

In a monodispersed sample, that is one in which all chains have the same molecular weight, the molecular weight averages are necessarily all equal. However, in a sample having a broader distribution of chain molecular weights, $\bar{M}_n < \bar{M}_v < \bar{M}_w < \bar{M}_z$, with $\bar{M}_z$ being biased in favour of the higher molecular weight species.

In previous papers [6, 24], it has been suggested that the higher molecular weight elements of the distribution may have a disproportionately greater influence on the toughness than those of a lower molecular weight. This seems reasonable in view of the proposed M^2 relationship of the fracture energy. For the above reasons, it was decided to use $\bar{M}_z$ as the measure of molecular weight of the samples.

8. Experimental determination of G_c

The load at fracture for each corresponding notch length was determined at a constant crosshead speed of 1.25 mm min^{-1} on an Instron testing machine in a three-point bend deformation mode, as in Fig. 5. The exact initial crack length was measured on the broken surface of the specimen using a travelling microscope. The modulus at each molecular weight was determined, again in three-point bending, by analysis of the load deflection curve of an unnotched specimen.

The geometry function, y, was calculated for a span-to-depth ratio, $S/d = 4$ using a fourth degree polynomial [25] of the form:

$$y = 1.93 - 3.07\left(\frac{c}{d}\right) + 14.53\left(\frac{c}{d}\right)^2 - 25.11\left(\frac{c}{d}\right)^3 + 25.8\left(\frac{c}{d}\right)^4 \quad (19)$$

The values of $\sigma^2 y^2$ were plotted against $1/c$ for each set of specimens and K_c was calculated from the slope of the curve. G_c was subsequently calculated using the measured values of K_c and E according to Equation 13.

9. Results and discussion

Fig. 6 shows a typical plot of $\sigma^2 y^2$ against $1/c$ and it can be seen that the curve is essentially linear.

Table I contains the results of K_c and G_c obtained for each set of specimens. The measured modulus was found to be reasonably constant over the whole range of molecular weights, having a value of approximately 3.0 GN m^{-2}. This value was

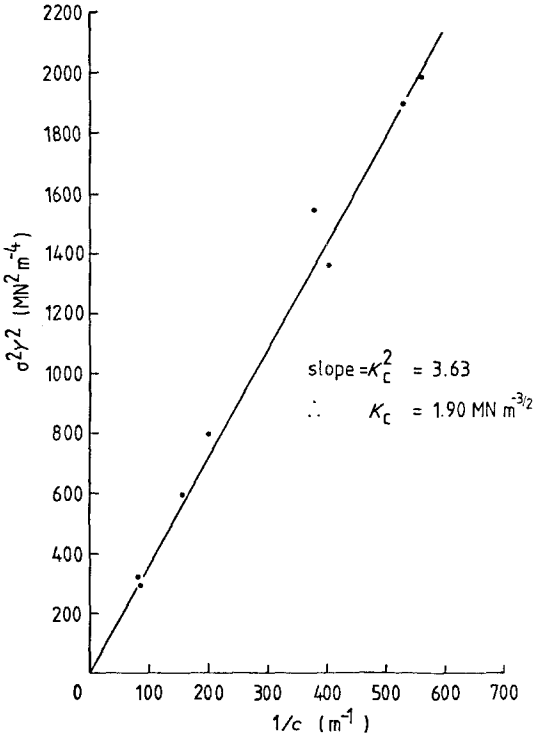

Figure 6 Typical plot of $\sigma^2 y^2$ against $1/c$ for the determination of K_c (Set C).

used along with K_c in Equation 13 to obtain G_c. It is worthy of note that the results obtained for G_c in three-point bending in the present study, appear to be at variance with those obtained by other workers [22]. One plausible explanation for this apparent discrepancy is that the data in the Kusy and Katz [22] study, obtained at low fracture rates by means of cleavage bar experiments, reflects the fracture toughness at the point of crack initiation (i.e. $K_c = 0.77\,\mathrm{MN\,m^{-3/2}}$ at $M > M_c$, assuming a modulus of $3\,\mathrm{GN\,m^{-2}}$). Whereas the data presented here are a measure of the toughness at instability ($K_c = 1.8\,\mathrm{MN\,m^{-3/2}}$ at $M > M_c$). (See, for example, Marshall *et al.* [26].)

Fig. 7 is a plot of G_c against molecular weight and it can be seen that the experimentally determined values fit a curve of the form:

$$G_c = Ax(M - M_e)^2 + (1 - x)B \qquad (20)$$

for the two extremes of $x = 1$ and $x = 0$ using the values of the constants $A = 2.5 \times 10^{-8}\,\mathrm{J\,m^{-2}}$ and $B = 1150\,\mathrm{J\,m^{-2}}$. M_e in this equation is the critical molecular weight for entanglement which is introduced to account for the fact that below this value the fracture parameters tend to zero.

$$M_e = 2M_e^* \qquad (21)$$

where M_e^* is the molecular weight between entanglement points. A value for M_e of 2.2×10^4 found by Gent and Thomas [15] for the zero strength molecular weight is used in this instance.

One implication of this agreement is that the parameter x is some measure of the extent of chain pull-out and that above a critical value of M_c, it reduces to zero. Whilst it is possibly true to say that below M_c all chains fail by a pull-out mechanism, the situation above M_c is probably more complex because of the location of the plane of fracture relative to the centre of the individual molecules and the polydispersity of the sample.

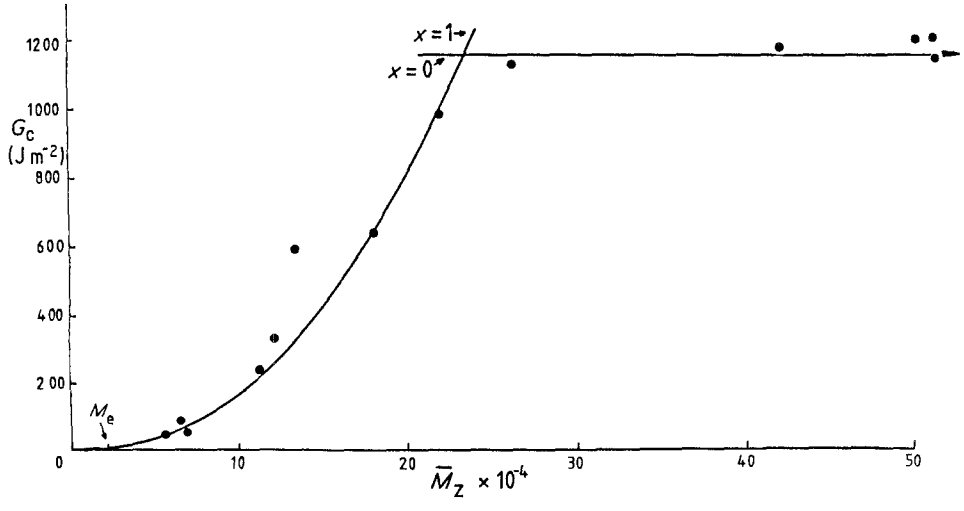

Figure 7 The critical energy release, G_c, as a function of molecular weight, $\bar{M}_z$. Experimental points are superimposed on the curve $G_c = Ax(M - M_e)^2 + (1 - x)B$, $A = 2.5 \times 10^{-8}\,\mathrm{J\,m^{-2}}$, $B = 1150\,\mathrm{J\,m^{-2}}$, and $M_e = 2.2 \times 10^4$.

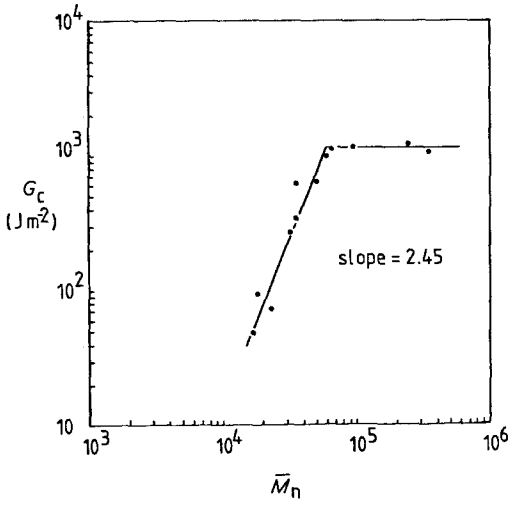

Figure 8 Log–log plot of G_c against $\bar{M}_n$. Slope = 2.45.

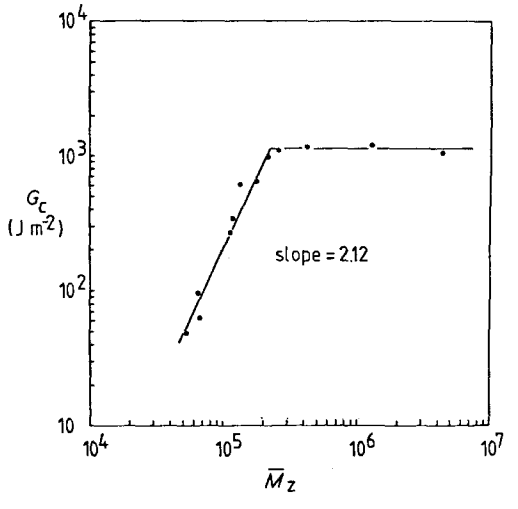

Figure 9 Log–log plot of G_c against $\bar{M}_z$. Slope = 2.12.

Because of the nature of the proposed model, not all chains of the same molecular weight will be embedded to the same extent on either side of the fracture plane; only those minimally crossing the plane would be expected to fail by a pull-out mechanism. Similarly, the shorter chains of the distribution would also disentangle in this manner. These proposals go a long way in explaining the fact that the measured fracture energy for the higher molecular weight samples is still very much higher than that which would be obtained by calculating the energy necessary to break all chains crossing a plane of unit area. This implies that even in these high molecular weight samples, there is a substantial amount of chain slippage during fracture.

Comparison of Figs. 8 and 9 demonstrates the influence of the chosen molecular weight averaging equation. A plot of log G_c against log M_n gives a slope of 2.45, whereas log G_c plotted as a function of log $\bar{M}_z$ results in a slope of 2.12.

It has been mentioned previously [6, 27] that the fully extended length of a PMMA chain of the experimentally determined critical molecular weight, which in the present case is about 2×10^5, is smaller than the measured value of the critical crack opening displacement (COD). However, it must be remembered that we are considering an average molecular weight and that a significant portion of the chains at the higher end of the molecular weight distribution will have lengths greater than the COD. At lower average molecular weights, there will be fewer of these longer chains so that the COD may also be expected to vary with molecular weight.

The COD, δ_c, has been shown to be a useful parameter for polymers and may be defined by the equation [20]:

$$\delta_c = \frac{G_c}{\sigma_c} \tag{22}$$

where σ_c is the craze stress.

From Equation 5, the force acting on the chains during the drawing stage in the formation of new surfaces, and hence the craze stress, is proportional to the length of the chains, and consequently to the molecular weight. This relationship has been found to hold reasonably well experimentally by Pitman and Ward [24] for polycarbonate (see Fig. 10). It has also been shown in the present work that $G_c \propto M_2$. Combining these two molecular weight relationships in Equation 2, it follows that:

$$\delta_c \propto M \tag{23}$$

The only data so far available for PMMA in which δ_c has been measured as a function of molecular weight are reported by Weidmann and Döll [28]. The values determined for the maximum thickness of the craze in their work are reproduced in Fig. 11 and, accepting the limited number of data points, there does seem to be a relationship of the form predicted below M_c. Above the critical molecular weight, the values of δ_c appear to be constant at about 2.7 μm. It is worthy of note that the value obtained for the critical molecular weight in the work of Weidmann and Döll was again in the region of 2×10^5. Additionally, extrapolation of the results for $M < M_c$ gives a value for the molecular weight at $\delta_c = 0$ of about

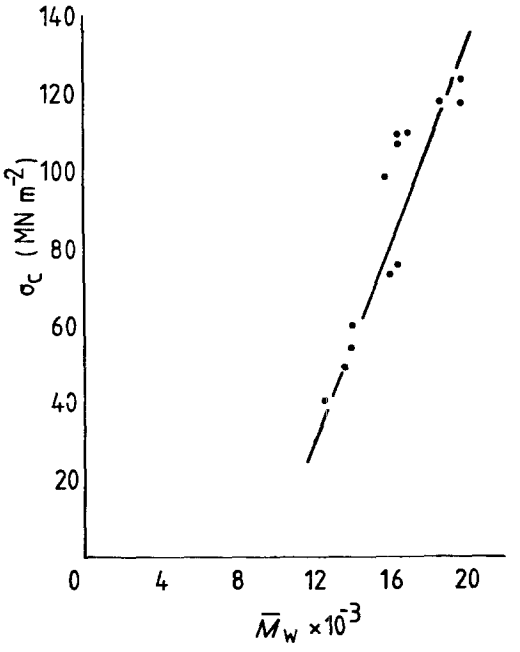

Figure 10 Craze stress against weight average molecular weight. Reproduced from Pitman and Ward [24].

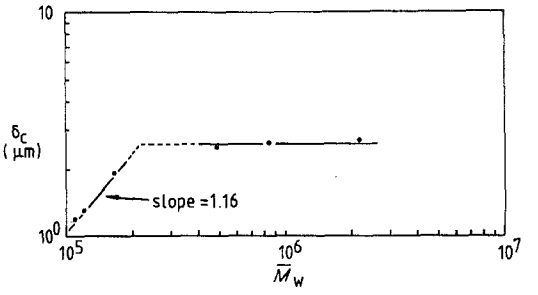

Figure 11 Log–log plot of COD against weight average molecular weight. Reproduced from Kusy and Turner [27].

2×10^4, which is of the same order as the critical molecular weight for entanglement formation. This also appears to be the case for polycarbonate [24] where extrapolation of the linear relationships of COD and craze stress against molecular weight result in a value of $\bar{M}_w$ at $\delta_c = 0$ and $\sigma_c = 0$ of about 10^4, a value which again is in the region of M_e for polycarbonate [29]. This seems reasonable since below M_e, in the absence of any substantial entanglements, the specimen may be expected to fail by a decohesion mechanism without the formation of a craze. Indeed, Pitman and Ward [24] state that below $\bar{M}_w = 1.2 \times 10^4$ for polycarbonate, there was no evidence of crazing on the fracture surface and that even very low loads caused unstable fracture and that razor notching was no longer possible.

10. Conclusion

Using the concept of linear elastic fracture mechanics, the toughness of PMMA has been determined from three-point bend tests using prenotched specimens. With this value of toughness and a measured value of the elastic modulus, which was found to remain almost constant over the whole molecular weight range, a value for the critical energy release rate, G_c, was calculated. A plot of G_c against molecular weight tended to support a relationship of the form $G_c \propto (M - M_e)^2$, up to a critical value of molecular weight, above which G_c was found to be constant. This relationship is compatible with a model for crack propagation in which polymer chains may be removed from the newly formed surface by a pull-out mechanism up to a critical chain length, above which scission becomes the preferred mode of chain failure. This latter proposal is in full agreement with a recently published observation [30] that significant chain scission occurs during crazing of polystyrene. The molecular weight and the molecular weight distribution were measured using GPC, before and after crazing, and it was found that the higher molecular weight chains underwent scission in preference to those of lower molecular weight.

Some evidence has been presented which tends to suggest that, in PMMA, the COD also increases linearly with increasing molecular weight up to a maximum value of molecular weight, above which it is constant.

Acknowledgements

The author wishes to thank Professor J. G. Williams and other members of the Strength of Materials Group at Imperial College for many stimulating discussions. Molecular weight determinations were kindly performed by the Polymer Supply and Characterisation Centre at RAPRA, and the generous help of Dr S. Holding is gratefully acknowledged. Irradiation of specimens was conducted by Mr Brian Bennett in the Chemical Engineering Department of Imperial College and his assistance is much appreciated. Financial support was from the SERC, which is also gratefully acknowledged.

References

1. J. P. BERRY, *J. Polymer Sci.* **50** (1961) 107.
2. *Idem, ibid.* **A2** (1964) 4069.

3. R. N. HAWARD, "The Physics of Glassy Polymers", edited by R. N. Haward (Applied Science Publishers Limited, London, 1973).
4. F. BEUCHE, "Physical Properties of Polymers" (Interscience Publishers Limited, New York, 1962).
5. B. H. BERSTED, *J. Appl. Polymer Sci.* **24** (1979) 37.
6. P. PRENTICE, *Polymer* **24** (1983) 344.
7. J. KLEIN and B. J. BRISCOE, *Proc. Roy. Soc.* **A365** (1979) 53.
8. W. W. GREASLEY, *Adv. Polymer Sci.* **16** (1974) 1.
9. H. R. BROWN and I. M. WARD, *Polymer* **14** (1973) 569.
10. A. J. KINLOCH, preprints "Micromechanics of Crack Extension", "Mechanics and Physics of Fracture II' Cambridge, March 1980, (Metals Society/Institute of Physics, London/Bristol, 1980).
11. A. M. DONALD and E. J. KRAMER, *Polymer* **23** (1982) 1183.
12. *Idem, J. Polymer Sci., Polymer Phys. Ed.* **20** (1982) 899.
13. E. J. KRAMER, *Adv. Polymer Sci.* **52/53** (1983) 1.
14. A. N. GENT, *J. Mater Sci.* **5** (1970) 925.
15. A. N. GENT and A. G. THOMAS, *J. Polymer Sci.* **10** (1972) 571.
16. A. S. ARGON and J. G. HANNOOSH, *Phil. Mag.* **36** (1977) 1195.
17. P. G. DE GENNES, *J. Chem. Phys.* **55** (1971) 572.
18. *Idem,* "Scaling Concepts in Polymer Physics" (Cornell University Press, Ithaca, London, 1979).
19. P. I. VINCENT, *Polymer* **13** (1972) 558.
20. J. G. WILLIAMS, *Adv. Polymer. Sci.* **27** (1978) 67.
21. ASTM D790-71 (1971).
22. R. P. KUSY and M. J. KATZ, *Polymer* **19** (1978) 1345.
23. M. DOLE, "The Radiation Chemistry of Macromolecules" (Academic Press, New York, London, 1973).
24. G. L. PITMAN and I. M. WARD, *Polymer* **20** (1979) 895.
25. W. F. BROWN and J. E. SRAWLEY, *ASTM STP 410* (1966) 1.
26. G. P. MARSHALL, L. H. COUTTS and J. G. WILLIAMS, *J. Mater Sci.* **9** (1974) 1409.
27. R. P. KUSY and D. T. TURNER, *Polymer* **18** (1977) 391.
28. G. W. WEIDMANN and W. DÖLL, *Colloid Polymer Sci.* **254** (1976) 205.
29. R. S. PORTER and J. F. JOHNSON, *Chem. Revs* **66** (1966) 1.
30. R. POPLI and D. ROYLANCE, *Polymer Eng. Sci.* **22** (1982) 1046.

Received 9 February
and accepted 4 June 1984